42nd AIAA/ASME/ASCE/AHS/ASC Structures, Structural Dynamics, and Materials Conference and Exhibit
Seattle, WA 16-19 April 2001

A01-25426

AIAA 2001-1582

CFD-BASED ANALYSIS OF NONLINEAR AEROELASTIC BEHAVIOR OF HIGH-ASPECT RATIO WINGS

M. J. Smith*, M. J. Patil†, D. H. Hodges**
Georgia Institute of Technology, Atlanta, GA 30332-0150

Abstract

A nonlinear aerodynamic methodology has been loosely coupled to a geometrically exact beam structural analysis to study the static aeroelastic behavior of a high-aspect-ratio wing. The aim of the present effort was to investigate the effects of adding aerodynamic nonlinearity on the elastic behavior, in particular identifying the areas of nonlinearities and their importance. Care was taken to evaluate the Euler solver and the transfer of data between the aerodynamic and structural modules to identify sources of numerical error that may contribute to incorrect modeling of large deflections. It was found that sensitivities near the wing tip and leading edge required additional attention when clustering the computational aerodynamic grid near the surface. Further, the transfer of loads from the Euler code to the structural code requires that the nonlinear drop of forces and moments be modeled as exactly as possible. Otherwise errors in the predicted geometric deformations of up to 10% can occur. These are exacerbated for cases with large deflections and twist. For loosely coupled static aeroelastic simulations, the nonlinear aerodynamic predictions provided by the solution of the Euler equations are lower than the predictions of the vortex panel code. This results in lower predicted bending and twist by the higher-order aerodynamic code, indicating that the divergence and possibly flutter speeds predicted by lower-order aerodynamics may be overly conservative.

* Assistant Professor, School of Aerospace Engineering, Associate Fellow AIAA
† Now Assistant Research Professor, Duke University, Member AIAA
** Professor, School of Aerospace Engineering, Fellow AIAA

Introduction

Fluid-Structure Interaction (FSI) has become an integral part of research development efforts as computational methods have matured. FSI is applicable to many engineering fields, and in conventional aerospace engineering applications, is known as aeroelasticity. The traditional definition of aeroelasticity assumes that the structure is inherently flexible, and the fluid (air) around it also becomes unsteady due to surface motion or fluid disturbances.

Numerical methods to simulate FSI have been under development for many years. These methods have typically concentrated on the structural aspects of the problem, using simple fluid mechanics methods to keep computational requirements reasonable for large numbers of parametric runs. FSI has been a focus of research efforts in the CFD community for only the past 12 years as computational methodologies have matured to a level of confidence where interdisciplinary problems may be tackled.

There has been a growing interest in vehicles, typically unmanned, that consist of high-aspect-ratio lifting surfaces of the order of up to 35. Large deflections up to 25% of the wing semi-span can result from the high flexibility and large aspect ratios of the wing. Patil et al[1] have examined the effect of structural geometric nonlinearities on the flutter behavior of high-aspect-ratio wings, demonstrating that there is a significant change in the structural frequencies and the aeroelastic response. Patil and Hodges[2] and Hall et al[3] have shown that lower-order theories also predict significant changes in the physics of large deformation in wings. Additional aerodynamic fidelity is necessary to capture the physics near stall and higher Mach numbers, as well as to capture viscous effects to compute drag.

Geometric Nonlinearities

Structural and aerodynamic geometric nonlinearities are based in the kinematic description of the body. The pressures, velocities, and strains on the wing should be defined in terms of the local displacement of the wing for both non-trivial steady-state and dynamic motion. These nonlinearities must be consistently applied in both the structural and aerodynamic models of the numerical analysis.

CFD-CSD Methodologies

There are three primary classes of Euler/Navier-Stokes-based FSI methodologies. The first class of methodologies is known as a fully-coupled analysis or unified fluid-structure interaction. These methods reformulate the governing equations so both the fluid and structural equations are combined into one set of equations. These new governing equations are solved and integrated in time simultaneously. An example of this application is the research code developed by Guruswamy[4]. This class of methodologies is not yet available in production FSI codes with high-order fluid mechanics load prediction capabilities.

The second class, and currently the most widely used, is a closely-coupled FSI analysis, examples of which include, for air-based applications, ENS3DAE[5], ENSAERO[6], and CFL3DAE[7]. The fluid mechanics and structural dynamics modules remain independent in their solutions, and their interaction is limited to the passage of surface loads and surface deformation information after each CFD time step or iteration.

The third class of methodologies is the loosely-coupled analysis. Here, CFD analyses are updated by structural deflections only after partial or full convergence. Thus grid deflection updates are performed sparingly, usually 3-10 times per analysis[8,9]. These computations have primarily been accomplished using CFD codes and external interpolation and loads calculation routines that are uncoupled.

These methods have been undergoing development and research applications for a number of years. Several proven methods exist and are used by government and industry to examine external aeroelastic problems, primarily wing-based aeroelastic issues [5,6,10,11] such as static aeroelasticity, aeroelastic tailoring, and limited flutter analysis.

The structural modeling on the other hand has developed over time from simple modal analysis[12] to detailed finite-element models[13]. Nonlinear structural dynamics and its effects on aeroelastic instabilities and limit-cycle oscillations has also been studied[14,15,16]. In most cases the nonlinear structural models were coupled with simple linear unsteady aerodynamic models and in some cases empirical ONERA stall model[17].

Investigational Procedure

The investigational procedure used here is to compute and compare various linear and nonlinear steady-state solutions of the aeroelastic system. These are accomplished using an Euler/Navier-Stokes computational fluid dynamics (CFD) method, ENS3DAE, coupled with an in-built linear structural model and the nonlinear structural model of Patil and Hodges[2]. The results generated by the present computational procedure will be used to validate earlier results[13,16] using linear aerodynamics models and to understand the numerical implications in performing this CFD-CSD coupling.

Numerical Modeling

Nonlinear Aerodynamic Model

The **E**uler/**N**avier-**S**tokes **3**-**D**imensional **A**ero**E**lastic, ENS3DAE, methodology was developed to examine a multitude of aeroelastic problems, primarily in the transonic flight regime. The solver was originally developed by the Lockheed-Georgia Company (now Lockheed-Martin Aeronautical Systems Group) for a variety of applications[18,19,20]. The solver was extended to consider aeroelasticity by Lockheed in 1990 under contract to the Air Force[5,21] and has been undergoing extensions to examine different types of aeroelastic problems since that time[22,23].

The aerodynamic module in ENS3DAE solves the full 3-D Reynolds-averaged Navier-Stokes equations for compressible flow, or simplifications thereof, including the thin shear layer Navier-Stokes and the Euler equations. Both implicit, time-accurate (fixed time step) or steady state (spatially varying time step) options are employed via a time-marching fully-implicit approximate

factorization scheme. Boundary conditions are applied explicitly along the faces of each zone. O-, C- and H- grid combinations can all be solved in this manner.

Linear & Nonlinear Structural Model

The structural model used in the present work is based on the mixed variational formulation for the dynamic of beams developed by Hodges[24]. Here, the wing is modeled as a geometrically-exact beam. Thus, the kinematics are accurate for large deformation of the wing and the model can be used for nonlinear structural simulation. By discretizing the problem and using simple shape functions, the mixed variational formulation leads to an efficient finite element based solution procedure[25]. For each finite element in the structural representation, the force (F), moment (M), displacement (u), rotation (θ), and velocity (V, Ω) equations for each node are:

$$\frac{F^{n+1}-F^{n}}{\Delta t}+f_{aero}+\tilde{\bar{\kappa}}^{n}\left(\frac{F^{n+1}+F^{n}}{2}\right)-\dot{P}^{n}=0$$

$$\frac{M^{n+1}-M^{n}}{\Delta t}+m_{aero}+\left(\tilde{e}_1+\tilde{\bar{\gamma}}^{n}\right)\left(\frac{F^{n+1}+F^{n}}{2}\right)+\tilde{\bar{\kappa}}^{n}\left(\frac{M^{n+1}+M^{n}}{2}\right)-\dot{H}^{n}=0$$

$$\frac{u^{n+1}-u^{n}}{\Delta L}+e_1-C^{is}\left(e_1+\bar{\gamma}^{n}\right)=0$$

$$\frac{\theta^{n+1}-\theta^{n}}{\Delta L}-\left(I+\frac{\tilde{\bar{\theta}}^{n}}{2}+\frac{\bar{\theta}^{n}\left(\bar{\theta}^{n}\right)^{T}}{4}\right)\bar{\kappa}^{n}=0 \qquad (1)$$

$$\dot{u}^{n}-C^{is}V^{n}=0$$

$$\dot{\theta}^{n}-\left(I+\frac{\tilde{\theta}^{n}}{2}+\frac{\theta^{n}\left(\theta^{n}\right)^{T}}{4}\right)\Omega^{n}=0$$

Here, $\bar{\gamma}$ and $\bar{\kappa}$, the strains and curvatures are related to the forces (F) and moments (M) by a cross-sectional constitutive law. P and H, the linear and angular momenta, are related to the linear and angular velocities (V and Ω) using the cross-sectional inertial properties

$$\begin{Bmatrix}\bar{\gamma}\\ \bar{\kappa}\end{Bmatrix}=[S]\begin{Bmatrix}\frac{F^{n}+F^{n+1}}{2}\\ \frac{M^{n}+M^{n+1}}{2}\end{Bmatrix}$$

$$\begin{Bmatrix}P\\ H\end{Bmatrix}=[I]\begin{Bmatrix}\frac{V^{n}+V^{n+1}}{2}\\ \frac{\Omega^{n}+\Omega^{n+1}}{2}\end{Bmatrix} \qquad (2)$$

The direction cosine matrix, C^{is}, is used to transform a vector from the deformed wing s-frame to the undeformed straight wing i-frame. f_{aero} and m_{aero} are the aerodynamic forces and moments acting on each element, and are computed using the Euler equations of motion within the CFD methodology.

This model was loosely coupled to the ENS3DAE methodology and was utilized in place of the original linear structural model for some computations.

Configuration

The goal of this work is study the impact of a higher-order computational aerodynamic methodology with a nonlinear wing structural model. The wing configuration that was used is a rectangular, untwisted wing with no sweep. The span consists of a NACA0012 airfoil from root to tip at a geometric angle of attack of zero degrees. Various flight conditions were simulated at varying angles of attack using both a rigid and flexible wing, structurally modeled as a nonlinear beam. For this paper, a standard atmosphere is used at an altitude of 20,000 m. Unless otherwise noted, the flight speed of the wing is 25 m/s. The structural properties of the wing are provided in Table 1.

Computational Grid

The computational grid was generated using an H-H grid generation program developed for ENS3DAE. This aerodynamic grid does not

contain any of the internal structure since the configuration of interest was the external flow fields over rigid planforms. After some initial grid evaluations, the selected grid consisted of two blocks that modeled the upper surface and flow field, and the lower surface and flow field. Each block consisted of 121 streamwise × 43 spanwise × 50 normal points. The grid uses 67 streamwise and 33 spanwise points on each of the upper and lower wing surfaces. An orthogonal view of the surface grid is pictured in Figure 1.

Results

The objectives of this research have been to analyze the elastic behavior of high-aspect-ratio wings when the fidelity of the aerodynamic model is increased. Comparisons with results obtained using lower order aerodynamics[2] are presented in increasing levels of complexity.

Grid Sensitivity Studies

As with any numerical method, the aerodynamic and structural modules are susceptible to numerical errors if the grids are not sufficiently refined to accurately capture the parameter variations. The aeroelastic simulations are adversely affected if the structural deflection or aerodynamic loads are not accurately predicted. Previous studies using the nonlinear structural module have defined the required number of finite elements. Nonlinear aerodynamic modules based on the Euler or Reynolds-Averaged Navier-Stokes CFD codes are known to be sensitive to the grid.

Aerodynamic Module: A typical rigid Euler grid was first evaluated for the overall accuracy of the lift and moment spanwise distributions. This grid applied moderate tip and leading edge clustering, and gives an overall lift distribution comparable to experimental values. However, the spanwise lift distribution at non-zero angles of attack was not accurate enough for use in this study, as seen in Figure 2. The lower lift distributions at the root are compensated farther out wing. The wing tip was modeled simply as a finite thickness with the upper and lower grid lines collapsing to a single grid line at the first spanwise station off the wing surface, as depicted in Figure 3. This generates a non-physical spike in the aerodynamic forces and moments for the wing station next to the tip, as seen in Figure 2. This spike has been shown[26] to not impact the aeroelastic simulation if it is located very close to the tip so that its impact on the forces and moments is minimized. The moderately clustered grid means that this spike occurs too far inboard, such that there is an impact on the aerodynamic loads.

Denser clustering was added at the leading edge to further capture the suction peak, as well as the tip. This grid provides a more physically correct lift and moment spanwise distribution, as well as moving the tip spike within 2% of the tip location (see Figure 2).

Data Interpolation: In addition to the aerodynamic and structural modules themselves, errors can be introduced when data is transferred between modules. This data transfer occurs twice: 1) forces and moments are passed from the aerodynamics module to the structural module, and 2) geometric deflections are passed from the structures module back to the aerodynamics module.

Consider the first case when forces and moments are passed from the aerodynamics module to the linear structural module. Because the large aspect ratio wing is considered to be a beam, the nonlinear structural model requires only the forces and moments at the midchord. As seen in Figure 3, the normal forces across the span for a flexible surface are nonlinear. The nonlinear structural module, as currently written, requires that the aerodynamic loads be passed as a set of equally-spaced spanwise values. This requires that some interpolation be performed on the aerodynamic output.

A simple piecewise-linear and a more complex polynomial fit were tested to determine the impact of the interpolation method on the resulting nonlinear structural deflections. There was little (<0.1%) difference in the resulting deflections for the same number of spanwise stations, provided that enough stations were utilized.

There is, however, a sensitivity related to the number of spanwise stations passed to the structural code. Given a set of 33 nonlinearly spaced spanwise points in the aerodynamic simulation, sets of 16, 32, and 64 points were evaluated using the lift force and pitching moment. As seen in Figure 3, the interpolated values of the normal force are indistinguishable when plotted on

the original CFD distribution. Comparisons of the overall piecewise integrated lift an 8%, 2.5%, and 1.2% difference with the piecewise integrated CFD lift for the 16, 32, and 64 points, respectively. When these lift forces, along with the pitching moment, are used to predict the beam deflection and twist, there exist up to 10% differences at the tip for one aeroelastic update. The differences between the 32 and 64 points are less than 2%, while further refinement to 80 points shows virtually no difference with the 64 point prediction. The difference in the simulations is directly traced to the nonlinear drop of the forces and moments near the tip. The removal of the nonlinear tip spike from the CFD data prior to the linear piecewise interpolation for up to 32 span points does not change the predicted deflections. If the calculation is continued to convergence for a static aeroelastic case (see case 1), the use of 16 spanwise points yielded an overall underprediction of 20% in the tip bending and 14% in the tip twist.

A prescribed deflection was evaluated to determine the appropriate number of spanwise stations necessary to define the CFD grid. It was determined that 16 to 20 stations is necessary to model the curvature of the wing.

Lift Distribution

The first case that was studied is that of a curved, rigid wing. The curved wing was generated by applying a distributed load on the flexible straight wing defined in Table 1 using the nonlinear geometric code of Patil[2]. This resulted in a wing deflection, w (calculated analytically from linear beam theory), described by

$$w = \frac{4}{3}\left(\frac{x}{L}\right)^2\left[6 - 4\frac{x}{L} + \left(\frac{x}{L}\right)^2\right] \qquad (3)$$

where L is the half-span of the wing. This resulted in a tip deflection of about 4 m, or 25% of the half-span, as shown in Figure 4. This configuration was utilized to determine the effect of the large curvature on the 3-D aerodynamic load characteristics. Care was taken in developing the wing geometry so that the full impact of the curvature over the wing was accounted in the final numerical grid.

Figure 5 shows the plot of lift distribution on this curved wing. The lift distribution has been nondimensionalized by the two-dimensional flat plate lift curve slope to enhance the comparison plot. Results shown also include the loads computed by Patil and Hodges using a panel method in Reference 2. The results from the Euler run have been interpreted and plotted in two different ways.

The lift direction is determined to the prescribed rigid angle of attack in steady cases or the prescribed time-dependent pitching angle in unsteady rigid simulations. This can also be used in flexible calculations for small tip deflections with very small errors. However, when the tip deflection becomes large, such as the example presented here, the lift can be overpredicted near the tip using this method. Instead, the lift should be referenced to the local normal at each span station.

This trend is similar to the observations of Patil and Hodges[2] using a panel method. As seen in Figure 3, the Euler-predicted lift drops off much closer to the tip than the panel method. This change in the three-dimensional effect is expected due to the dense Euler grid and the higher fidelity of the aerodynamics. The Euler computation experiences a maximum 5% reduction in the lift for this case. A series of Mach numbers was run from M_∞=0.1 to 0.9. The difference in the two lift distributions remained at a maximum of about 5% throughout this Mach regime.

Static Aeroelasticity

The undeflected wing was run at an equivalent altitude of 20,000 meters and a flight speed of 25 m/s. Two cases were simulated at angles of attack at two (2) and four (4) degrees using both linear and nonlinear structural models. These simulations were computed in the following manner:

1) The flight loads and moments on the wing were computed at the midchord of each aerodynamic node location using the Euler option of the ENS3DAE code.
2) These values were interpolated to equal spanwise locations along the span.
3) The linear or nonlinear structural model provided equally spaced deflections based on these aerodynamic inputs.
4) A new grid was generated for these deflections.

5) Steps 1 - 3 were repeated until the tip deflection and twist did not change more than 2% between iterations. This usually occurred within 4 - 6 aeroelastic updates, as seen in Figure 6.

The first static aeroelastic case considered was a cruise-compatible flight condition. The flight speed was 25 m/s at 20,000 m altitude at an angle of attack of 2°. Figure 7 shows a comparison of three different aeroelastic solutions. The original run used a vortex lattice panel code to predict the aerodynamics. Patil and Hodges[2] showed that the nonlinear structures played little if any role at this flight condition. When nonlinear aerodynamics is added in the form of the solution of the Euler equations, there is a 8.5 to 12% difference in the predicted force, deflection and twist over the wing span. The nonlinear structural model increases the wing bending by 2% and the wing twist by less than 1% over the linear structural model. Overall, it is evident that the introduction of the Euler-based aerodynamics reduces the aeroelastic behavior of the wing. This is due to the lower flight loads and slightly different distribution of them over the wing.

The second case considered is a flight condition resulting in a larger aeroelastic response. The flight speed was 25 m/s at 20,000 m altitude at an angle of attack of 4°. Figure 8 shows a comparison of three different aeroelastic solutions. The trends observed for the 2° angle of attack case are repeated here, but the differences are magnified. The force distribution for the Euler solutions is slightly different than the panel distribution, and the maximum is 20% less than the panel code maximum. The Euler prediction of the tip bending of the wing is 11% less than the panel code, while the twist prediction is 20% less. The linear structural model tip bending prediction appears to be slightly (2%) closer to the panel code - nonlinear model prediction because the bending dihedral angle is not accounted for in the linear model. However, it is clear from Figure 8 that this is not the case, and there exists close to a 5% difference. The tip twist is almost identical for the nonlinear and linear structural model using the Euler aerodynamic model.

Conclusions

A method based on nonlinear structural beam theory has been loosely coupled with an Euler-based aerodynamics code to study large aspect ratio wings. The role of physics associated with the nonlinear aspects of the simulation has been identified and evaluated. Assumptions made during the development or application of numerical methods that utilize nonlinear methods must be re-evaluated for wings with large aspect ratios. Geometric nonlinearities can change the aerodynamic loads up to 5%, leading to comparable errors in the static aeroelastic predictions. The accurate transfer of the loads to the structural model is especially sensitive to changes in curvature. A 10% error in deflection can yield a converged static aeroelastic error of 20% underprediction. A structural model that can handle clustered aerodynamic force and moment inputs and provide deflection updates that locally adapt to curvature are recommended for efficient practice.

The addition of a nonlinear aerodynamic model provides some three-dimensional relief in the loads, resulting in 10 - 15% lower deflections. For these nonlinear aerodynamic simulations, the linear structural model underpredicts the tip bending and twist values by 3 - 5%. Thus, the utilization of linear aerodynamic models may cause overly conservative predictions in divergence and flutter speeds.

Future work will include the tight coupling of these two methods to quantify the impact of the nonlinear aerodynamics model on the divergence and flutter speeds of large aspect ratio wings.

Acknowledgments

This research was supported in part by the U.S. Air Force Office of Scientific Research, USAF, under grant F49620-98-1-0032 (Maj. Brian P. Sanders, technical monitor). The views and conclusions contained herein are those of the authors and should not be interpreted as necessarily representing the official policies or endorsement, either expressed or implied, of AFOSR or the U.S. Government. The authors would like to thank Mr. Larry Huttsell of the Air Force Research Laboratory, Dr. David Schuster of NASA Langley Research Center, and Dr. Joe Vadyak of Lockheed-Martin for their insightful comments and suggestions in utilizing ENS3DAE.

References

1 Patil, M. J., Hodges, D. H., and Cesnik, C. E. S., "Characterizing the Effects of Geometrical Nonlinearities on Aeroelastic Behavior of High-Apect-Ratio Wings," In *Proceedings of the International Forum on Aeroelasticity and Structural Dynamics*, June 22-25, 1999, pg. 501-510.

2 Patil, M. J., and Hodges, D. H., "On the Importance of Aerodynamic and Structural Geometrical Nonlinearities in Aeroelastic Behavior of High-Aspect-Ratio Wings," AIAA Paper 2000-1448, AIAA/ASME/AHS Adaptive Structures Forum, April 2000.

3 Hall, B. Preidikman, S., and Mook, D. T., "A Time-Domain Simulation for Evaluating Smart Wing Concepts for Reducing Gust Loads," presented at the 1999 ASME Mechanics and Materials Conference, Blacksburg, VA, June 1999.

4. Guruswamy, G. P., and Byun, C., "Fluid-Structural Interactions Using Navier-Stokes Flow Equations Coupled with Shell Finite Element Structures," AIAA Paper 93-3087, 24th Fluid Dynamics Conference, July 1993, Orlando, FL.

5. Schuster, D. M., Vadyak, J. and Atta, E., "Flight Loads Prediction Methods for Fighter Aircraft," WRDC-TR-89-3104, Nov., 1989.

6. Byun, C. and Guruswamy, G. P., "A Comparative Study of Serial and Parallel Aeroelastic Computations of Wings," NASA Technical Memorandum 108805, Jan. 1994.

7. Robinson, B. A., Batina, J. T., Yang, H. T. Y., "Aeroelastic Analysis of Wings Using the Euler Equations with a Deforming Mesh," *Journal of Aircraft*, Vol. 28, No. 11, November 1991, pp. 781-788.

8. Smith, M. J., Huttsell, L., Schuster, D. M., and Buxton, B., "Development of an Euler/Navier-Stokes Aeroelastic Method for Three-Dimensional Vehicles with Multiple Flexible Surfaces," AIAA Paper No. 96-1513, presented at the 37th Structures, Structural Dynamics, and Materials Conference, April 15-17, 1996.

9. Smith, M. J., "Computational Considerations of an Euler/Navier-Stokes Aeroelastic Method for a Hovering Rotor", *Journal of Aircraft.*, Vol. 33, No. 2, March-April 1996, pg. 429-434.

10. Rickets, R. H., Noll, T. E., Whitlow, W., and Huttsell, L. J., "An Overview of Aeroelasticity Studies for the National Aero-Space Plane," AIAA Paper No. 93-1313, April 1993.

11. Melville, R. and Gordnier, R., "Numerical Simulation of Large Amplitude Aeroelastic Wing Response," AIAA Paper No. 98-2657, June 1998.

12. Goland, M., "The Flutter of a Uniform Cantilevered Wing," *Journal of Applied Mechanics*, Vol. 12, No. 4, Dec 1945, pp. 197 - 208.

13. Patil, M. J., Hodges, D. H., and Cesnik, C. E. S., "Nonlinear Aeroelasticity and Flight Dynamics of High-Altitude, Long-Endurance Aircraft," Proceedings of the 40th Structures, Structural Dynamics, and Materials Conference, St. Louis, MO, Apr. 1999, AIAA Paper 99-1470.

14. Dunn, P., Dugundji, J., "Nonlinear Stall Flutter and Divergence Analysis of Cantilevered Graphite/Epoxy Wings," *AIAA Journal,* V30, No. 1, Jan 1992, p. 153–162.

15. Tang, D. M. and Dowell, E. H., "Experimental and Theoretical Study for Nonlinear Aeroelastic Behavior of a Flexible Rotoe Blade," *AIAA Journal*, Vol. 31, No. 6, June 1993, pp. 1133 – 1142.

16. Patil, M. J., Hodges, D. H., and Cesnik, C. E. S., "Limit Cycle Oscillations in High-Aspect-Ratio Wings," In Proceedings of the 40th Structures, Structural Dynamics, and Materials Conference, Saint Louis, Missouri, April 1999, AIAA Paper 99-1464.

17. Tran C. T. and Petot, D., "Semi-Empirical Model for the Dynamic Stall of Airfoils in View of the Application to the Calculation of Responses of a Helicopter Blade in Forward Flight," *Vertica*, V. 5, No. 1, 1981, p. 35–53.

18. Vadyak, J. and Smith, M. J., "Simulation of Engine Installation Flowfields Using a Three-Dimensional Euler/Navier-Stokes Algorithm," AIAA-86-1537, presented at the AIAA/ASME/SAE/ASEE 22nd Joint Propulsion Conference, Huntsville, AL, June 1986.

19. Vadyak, J., Smith, M. J., Schuster, D. M., and Weed, R., "Simulation of External Flowfields Using a 3-D Euler/Navier-Stokes Algorithm," AIAA-87-0484, presented at the 25th Aerospace Sciences Meeting, Reno, NV, Jan. 1987.

20. Vadyak, J., Smith, M., Schuster, D., and

Shrewsbury, G., "Simulation of Aircraft Component Flowfields Using a Three-Dimensional Navier-Stokes Algorithm," 3rd International Symposium on Science and Engineering on Cray Supercomputers, Cray Research, Inc., Minneapolis, MN, September 1987.

21. Schuster, D. M., Vadyak, J. and Atta, E., "Static Aeroelastic Analysis of Fighter Aircraft Using a Three-Dimensional Navier-Stokes Algorithm," AIAA-90-0435, presented at the 28th Aerospace Sciences Meeting, Reno, NV, January 1990. Also, *Journal of Aircraft*, Vol. 27, No. 9, pp. 820-825, September 1990.
22. Schuster, D. M., "Application of a Navier-Stokes Aeroelastic Method to Improve Fighter Wing Performance at Maneuver Flight Conditions," AIAA Paper No. 93-0529, presented at the 31st Aerospace Sciences Meeting and Exhibit, Reno NV, January 1993.
23. Smith, M. J., Schuster, D. M., Huttsell, L., Buxton, B., "Development of an Euler/Navier-Stokes Aeroelastic Method for Three-Dimensional Vehicles with Multiple Flexible Surfaces", AIAA Paper No. 96-1400, presented at the Structural Dynamics and Materials Meeting, Salt Lake City, UT, April 1996.
24. Hodges, D. H., "A Mixed Variational Formulation Based on Exact Intrinsic Equations for Dynamics of Moving Beams," *International Jour. of Solids and Structures*, Vol. 26, No. 11, 1990, p. 1253-1273.
25. Hodges, D. H., Shang, X., and Cesnik, C. E. S., "Finite Element Solution of Nonlinear Intrinsic Equations for Curved Composite Beams," *Journal of the American Helicopter Society*, Vol. 41, No.4, 1996, p. 313 –321.
26. Schuster, D. M., Private comm., April 2001.

Table 1. Structural Properties of the Wing

Wing Property	Study Value
Half Span	16 m
Chord	1 m
Mass per unit length	0.75 kg/m
Moment of inertia about the mid-chord	0.1 kg m
Spanwise elastic axis	0.5c
Center of gravity	0.5c
Bending rigidity	2×10^4 N m^2
Torsional rigidity	1×10^4 N m^2
Edgewise bending rigidity	5×10^6 N m^2

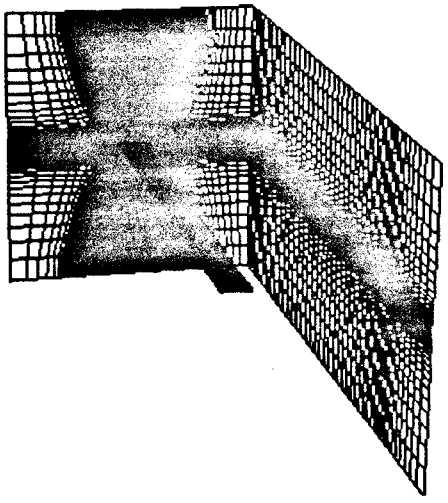

Figure 1. Orthogonal view of the test wing grid.

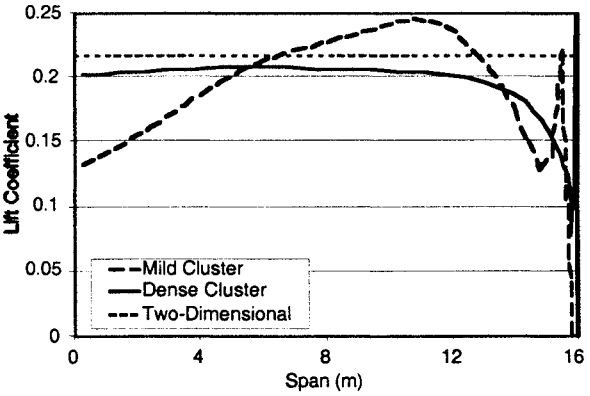

Figure 2. Spanwise lift distribution for different aerodynamic grid clustering, as predicted using the Euler equations of motion.

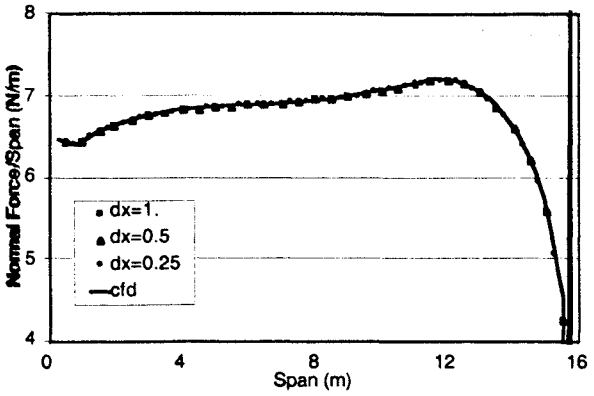

a) Interpolated normal force

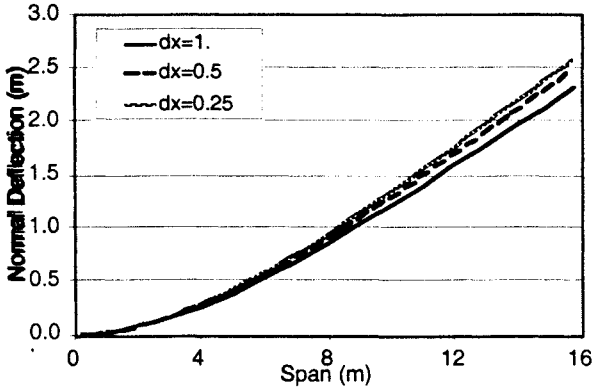

b) Nonlinear deflection predictions

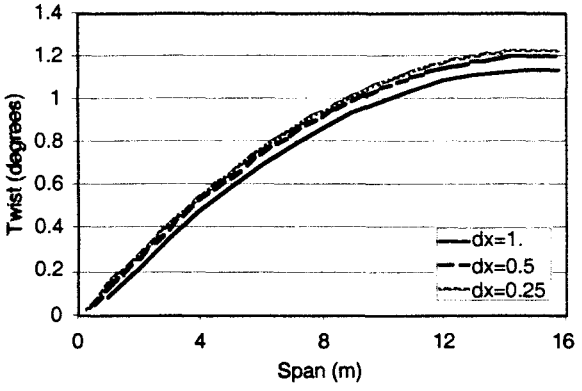

c) Nonlinear twist predictions

Figure 3. Spanwise lift distribution for different aerodynamic grid clustering, as predicted using the Euler equations of motion.

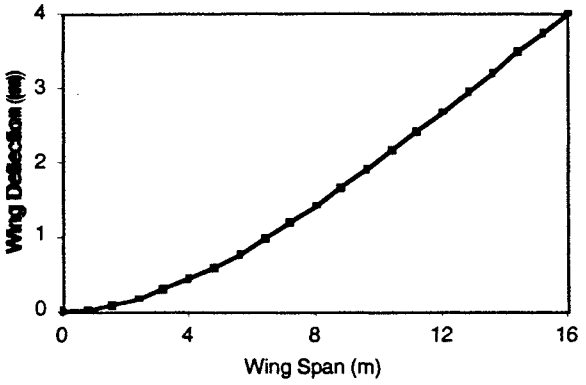

Figure 4. Curved wing using in steady-state calculations

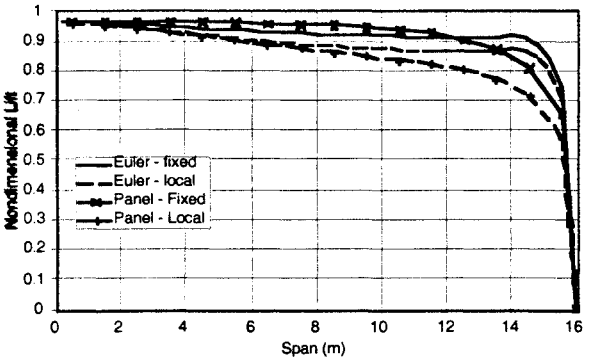

Figure 5. Lift distributions over a curved rigid wing

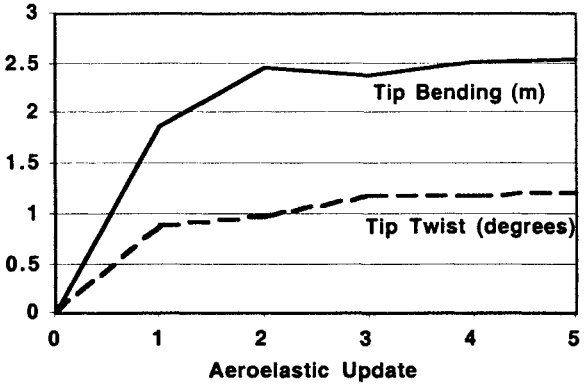

Figure 6. Loosely coupled aeroelastic solutions were considered converged when deflections changed less than 2% between aeroelastic updates

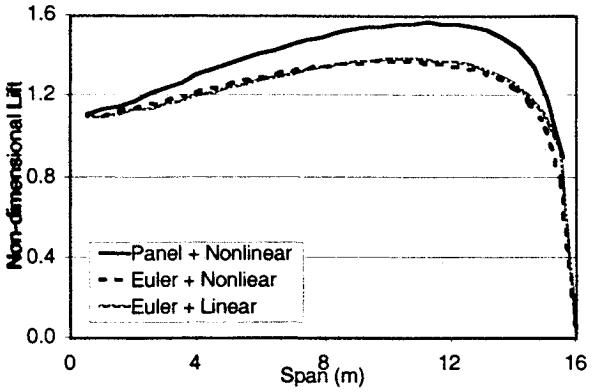

a) Nondimensional lift force

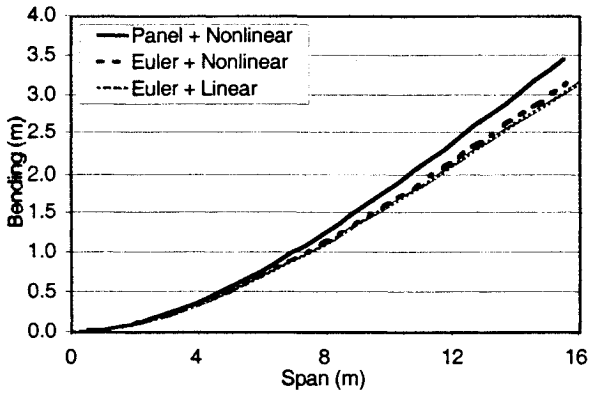

b) Bending

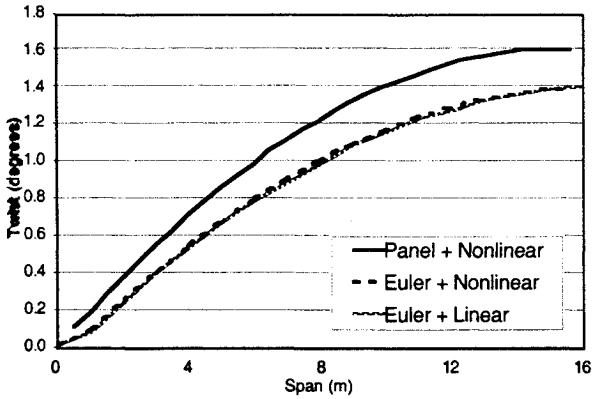

c) Twist

Figure 7. Static aeroelastic solution for a flight condition of 20,000 m altitude, 25 m/s, and an α=2°.

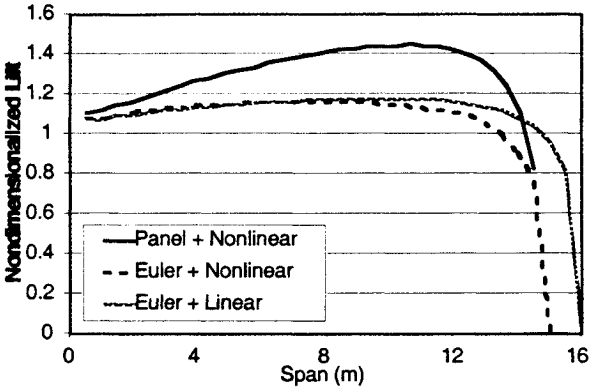

a) Nondimensional lift force

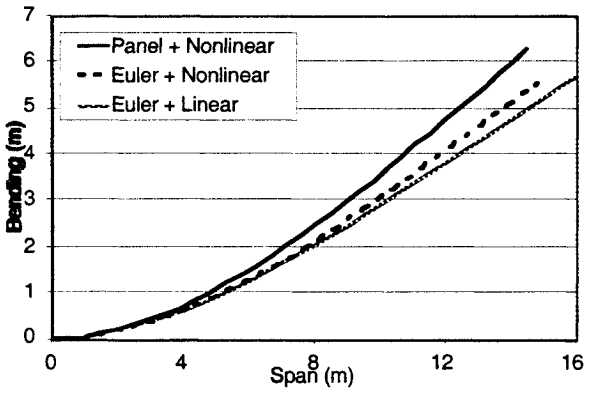

b) Bending

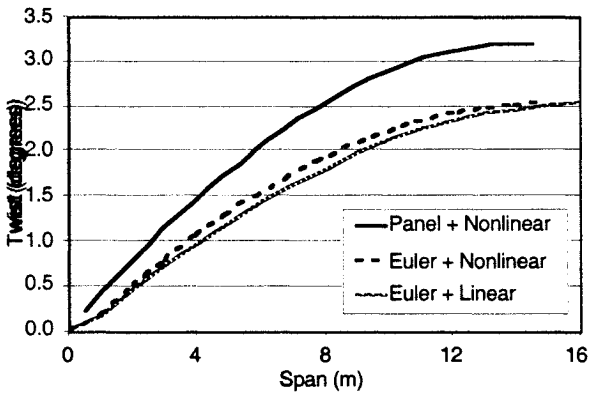

c) Twist

Figure 8. Static aeroelastic solution for a flight condition of 20,000 m altitude, 25 m/s, and an α=4°.